

Ordered Morphologies of Confined Diblock Copolymers

Yoav Tsori and David Andelman

School of Physics and Astronomy

Raymond and Beverly Sackler Faculty of Exact Sciences

Tel Aviv University, 69978 Ramat Aviv, Israel

ABSTRACT

We investigate the ordered morphologies occurring in thin-films diblock copolymer. For temperatures above the order-disorder transition and for an arbitrary two-dimensional surface pattern, we use a Ginzburg-Landau expansion of the free energy to obtain a linear response description of the copolymer melt. The ordering in the directions perpendicular and parallel to the surface are coupled. Three dimensional structures existing when a melt is confined between two surfaces are examined. Below the order-disorder transition we find tilted lamellar phases in the presence of striped surface fields.

INTRODUCTION

The self-assembly of block copolymers (BCP) has been the subject of numerous studies [1]-[12]. These macromolecules are made up of chemically distinct subunits, or blocks, linked together with a covalent bond. This bonding inhibits macrophase separation, and leads to formation of mesophases with typical size ranging from nanometers up to microns. For di-block copolymers, which are made up of two partially incompatible blocks (A and B), the phase diagram is well understood [1]-[6], and exhibits disordered, lamellar, hexagonal and cubic micro-phases. The phase behavior is governed by three parameters: the chain length $N = N_A + N_B$, the fraction $f = N_A/N$ of the A block, and the Flory parameter χ , being inversely proportional to the temperature.

The presence of a confining surface leads to various interesting phenomena [7]-[17]. The surface limits the number of accessible chain configurations and thus may lead to chain frustration. Transitions between perpendicular and parallel lamellar phases with respect to the confining surfaces have been observed in thin films [18]-[22]. In addition, the surface may be chemically active, preferring adsorption of one of the two blocks, and usually stabilizing the formation of lamellae parallel to the surface [12, 19, 21].

More complicated behavior occurs when the surface is chemically heterogeneous; namely, one surface region prefers one block while other regions prefer the second block. Compared to bulk systems, new energy and length scales enter the problem adding to its complexity. Thin-film BCP in presence of chemically patterned surfaces is of importance in many applications, such as dielectric mirrors and waveguides [23], anti-reflection coating for optical surfaces [24] and fabrication of nanolithographic templates [25].

THE MODEL

The copolymer order parameter ϕ is defined as $\phi(\mathbf{r}) \equiv \phi_A(\mathbf{r}) - f$, the deviation of the local A monomer concentration from its average f . Consider a symmetric ($f = 1/2$) BCP melt in its disordered phase (above the bulk ODT temperature) and confined by one or two flat, chemically patterned surfaces. The free energy (in units of the thermal energy $k_B T$) can be written as [3, 4, 5, 26, 27]:

$$F = \int \left\{ \frac{1}{2} \tau \phi^2 + \frac{1}{2} h [(\nabla^2 + q_0^2) \phi]^2 + \frac{u}{4!} \phi^4 - \mu \phi \right\} d^3 \mathbf{r} \quad (1)$$

The polymer radius of gyration R_g sets the periodicity scale $d_0 = 2\pi/q_0$ via the relation $q_0 \simeq 1.95/R_g$. The chemical potential is μ and the other two parameters are $h = 1.5\rho c^2 R_g^2/q_0^2$ and $\tau = 2\rho N(\chi_c - \chi)$. The Flory parameter χ measures the distance from the ODT point ($\tau = 0$), having the value $\chi_c \simeq 10.49/N$. For positive $\tau \sim \chi_c - \chi$, the system is in the disordered phase having $\phi = 0$, while for $\tau < 0$ (and $f = 1/2$) the lamellar phase has the lowest energy. Finally, $\rho = 1/Na^3$ is the chain density per unit volume, and c and u/ρ are constants of order unity [4]. This Ginzburg-Landau expansion of the free energy in powers of ϕ and its derivatives can be justified near the critical point, where $\tau \ll hq_0^4$ and ordering is weak. The lamellar phase can approximately be described by a single q -mode there: $\phi = \phi_q \cos(\mathbf{q}_0 \cdot \mathbf{r})$. We note that similar types of energy functionals have been used to describe bulk and surface phenomena [28, 29, 30], amphiphilic systems [31, 32], Langmuir films [33] and magnetic (garnet) films [34].

We model the chemically heterogeneous surfaces by a short-range surface interaction, where the BCP concentration at the surface is coupled linearly to a surface field $\sigma(\mathbf{r}_s)$:

$$F_s = \int \sigma(\mathbf{r}_s) \phi(\mathbf{r}_s) d^2 \mathbf{r}_s \quad (2)$$

The vector $\mathbf{r} = \mathbf{r}_s$ defines the position of the confining surfaces. Preferential adsorption of the A block is modeled by a $\sigma < 0$ surface field, and a constant σ results in a parallel-oriented lamellar layers (a perpendicular orientation of the chains). Without any special treatment, the surface tends to prefer one of the blocks, but by using random copolymers [16, 17] one can reduce this affinity or even cancel it altogether. A surface with spatially modulated pattern, $\sigma(\mathbf{r}_s) \neq 0$, induces preferential adsorption of A and B blocks to different regions of the surface.

RESULTS AND DISCUSSION

We consider first a system of polymer melt in contact with a single flat surface. The system is assumed to be above the ODT temperature, in the disordered bulk phase. The results are then extended to two confining surfaces and to BCP systems below the ODT.

Above ODT

Above the ODT the bulk phase is disordered, and the free energy, Eq. (1), is convex to second order in the order parameter ϕ . Thus, the ϕ^4 term can be neglected. The melt is

confined to the semi-infinite space $y > 0$, bounded by the $\mathbf{r}_s = (x, y = 0, z)$ surface. The chemical pattern $\sigma(\mathbf{r}_s) = \sigma(x, z)$ can be decomposed in terms of its inplane q -modes $\sigma(x, z) = \sum_{\mathbf{q}} \sigma_{\mathbf{q}} \exp(i(q_x x + q_z z))$, where $\mathbf{q} \equiv (q_x, q_z)$, and $\sigma_{\mathbf{q}}$ is the mode amplitude. Similarly, the order parameter is $\phi(x, y, z) = \sum_{\mathbf{q}} \phi_{\mathbf{q}}(y) \exp(i(q_x x + q_z z))$. Substituting ϕ in Eq. (1), and applying a variational principle with respect to $\phi_{\mathbf{q}}$, results in a linear fourth-order differential equation [35, 36]:

$$\left(\tau/h + (q^2 - q_0^2)^2\right) \phi_{\mathbf{q}}(y) + 2(q_0^2 - q^2) \phi_{\mathbf{q}}''(y) + \phi_{\mathbf{q}}''''(y) = 0 \quad (3)$$

In the semi-infinite geometry, $y > 0$, the solution to Eq. (3) has an exponential form $\phi_{\mathbf{q}}(y) = A_{\mathbf{q}} \exp(-k_{\mathbf{q}} y) + B_{\mathbf{q}} \exp(-k_{\mathbf{q}}^* y)$, where $k_{\mathbf{q}}$ is given by

$$\begin{aligned} k_{\mathbf{q}}^2 &= q^2 - q_0^2 + i\sqrt{\tau/h} \\ &= q^2 - q_0^2 + i\alpha(N\chi_c - N\chi)^{1/2} \end{aligned} \quad (4)$$

with $\alpha \simeq 0.59q_0^2$. The values of $\xi_q = 1/\text{Re}(k_{\mathbf{q}})$ and $\lambda_q = 1/\text{Im}(k_{\mathbf{q}})$ correspond to the exponential decay and oscillation lengths of the surface q -modes, respectively. For fixed χ , ξ_q decreases and λ_q increases with increasing q [20, 35, 36]. Close to the ODT (but within the range of validity of the model), and for q -modes such that $q > q_0$ we find finite ξ_q and $\lambda_q \sim (\chi_c - \chi)^{-1/2}$. The propagation of the surface imprint (pattern) of q -modes with $q < q_0$ into the bulk can persist to long distances, in contrast to surface patterns with $q > q_0$ which decays off close to the surface. This is seen by noting that q -modes in the band $0 < q < q_0$ are equally ‘‘active’’, i.e., these modes decay to zero very slowly in the vicinity of the ODT as $y \rightarrow \infty$: $\xi_q \sim (\chi_c - \chi)^{-1/2}$ and λ_q is finite.

The boundary conditions for $\phi_{\mathbf{q}}$ at $y = 0$ are

$$\begin{aligned} \phi_{\mathbf{q}}''(0) + (q_0^2 - q^2) \phi_{\mathbf{q}}(0) &= 0 \\ \sigma_{\mathbf{q}}/h + (q_0^2 - q^2) \phi_{\mathbf{q}}'(0) + \phi_{\mathbf{q}}'''(0) &= 0 \end{aligned} \quad (5)$$

The amplitude A_q is found to be $A_q = -\sigma_q \left(2\text{Im}(k_q)\sqrt{\tau h}\right)^{-1}$. Thus, the copolymer response diverges upon approaching the critical point as $(N\chi_c - N\chi)^{-1/2}$.

Although our analysis allows for arbitrary surface patterns, let us consider first the simple case of a surface attractive for the A block, but which has a single localized stripe, or surface ‘‘disturbance’’, preferentially attracting the B block (see Fig. 1 (a)). Far from this stripe A-blocks are adsorbed on the surface and the copolymer concentration profile has decaying lamellar order as was explained above. However, a non-trivial BCP morphology appears close to the stripe, reflecting the adsorption of B monomers. This behavior is indeed seen in Fig. 1 (b), where the grey scale is such that A-rich regions are white, while B-rich are black. A somewhat different situation is shown in Fig. 2 (a), where the black stripe is still preferential to the B monomers, but the rest of the surface (in grey) is neutral, $\sigma(x, z) = 0$. In this case no lamellar ordering parallel to the surface is expected. In (b) curved lamellae appear around the surface disturbance, optimizing interfacial energy. These curved lamellae are exponentially damped both in directions parallel and perpendicular to the surface. Clearly, the ordering in the perpendicular and lateral directions are coupled.

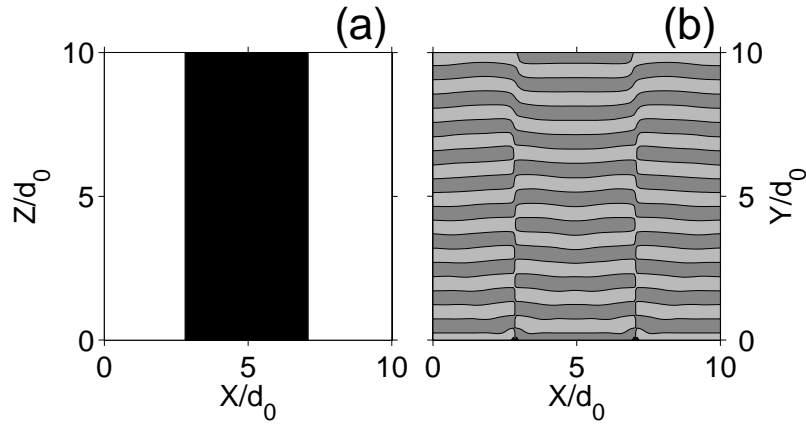


Figure 1. A BCP melt confined by one patterned surface having a central stripe of width $5d_0$. In (a) the surface located at $y = 0$ has a localized “surface disturbance” of $\sigma = 1/2$ inside the black stripe, favoring the adsorption of the B monomers, and $\sigma = -1/2$ outside of the stripe (favoring A monomers). The morphology in the x - y plane is shown in (b), where farther away from the stripe (large $y \gg d_0$) the lamellae have a decaying order, while close to the surface ($y \lesssim d_0$) the lamellae are distorted to optimize the interfacial energy. The system is above the ODT with $\chi N = 10$. Lengths are scaled by d_0 , the lamellar periodicity. B-rich regions are mapped to black shades and A-rich to white. In all plots we set the monomer length as $a = 1$, and choose in Eq. (1) $c = u/\rho = 1$, $R_g^2 = \frac{1}{6}Na^2$ and $N = 1000$ to give $\alpha \simeq 0.59q_0^2$.

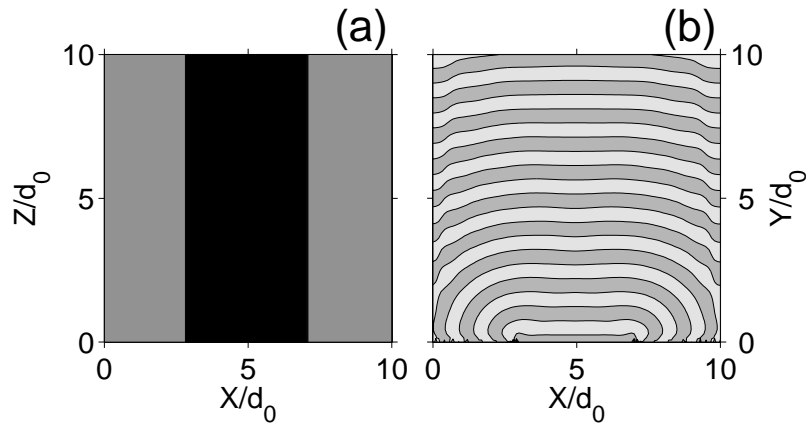


Figure 2. Same as in Fig. 1, but here the surface area outside of the stripe is neutral to polymer adsorption, $\sigma = 0$. The B monomers are found close to the stripe, inducing a curved lamellar structure that decays away from the surface.

A different scenario is presented in Fig. 3, where the surface has a sinusoidal variation in its affinity for the monomer type: $\sigma(x) = \sigma_0 + \sigma_q \cos(qx)$, with periodicity $d = 2\pi/q$ and average attraction $\langle \sigma \rangle = \sigma_0 > 0$ for the B monomers. The modulated surface field of amplitude σ_q induces lateral order, with A- and B-rich regions near the surface. Near the top of the figure ($y \gg d_0$), only lamellar-like ordering is seen, because the σ_q ($q > 0$) term decays faster than the σ_0 ($q = 0$) term.

Using this formulation, any two-dimensional chemical pattern $\sigma(x, z)$ can be modeled. For surface feature of size larger than d_0 , the characteristic copolymer length, the chemical surface

pattern can propagate via the BCP melt into the bulk. To demonstrate this we take in Fig. 4 (a)

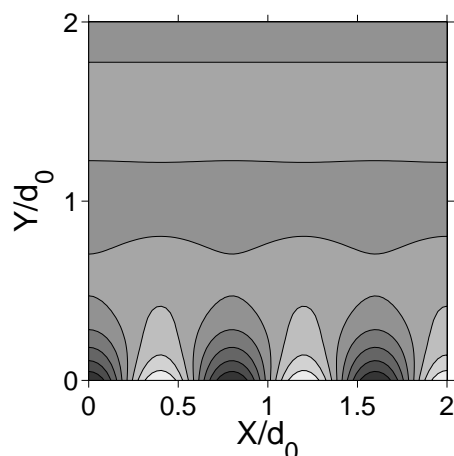


Figure 3. Copolymer morphology for a melt confined by one surface at $y = 0$ having a chemical affinity of the form $\sigma(x) = \sigma_0 + \sigma_q \cos(q_x x)$, with $q_x = \frac{5}{4}q_0$ and $\sigma_0 = \sigma_q = 0.1$. The lamellar-like order due to the σ_0 term persists farther away from the wall than the lateral order due to the σ_q term. The Flory parameter is $\chi N = 10.4$.

a surface pattern in the shape of the letters ‘MRS’. Inside the letters $\sigma > 0$ (B monomers are attracted), while for the rest of the surface $\sigma = 0$ (neutral). The resulting patterns in the x - z planes are shown for $y/d_0 = 0.5, 2$ and 3.5 in (b), (c) and (d), respectively. An overall blurring of the image is seen as the distance from the surface is increased. The fine details (e.g. sharp corners of the letters) disappear first as a consequence of the fast decay of high surface q -modes. The second point to notice is the $A \leftrightarrow B$ interchange of monomers that occurs for surfaces separated roughly by a distance of $(n + \frac{1}{2})d_0$, for integer n . This monomer interchange mimics the formation of lamellae in the bulk, although the temperature here is above the ODT. In addition, the appearance of lateral order is clearly seen, as lamellae form parallel to the edges of the letters.

We briefly mention the case where a BCP melt is confined between two flat parallel surfaces located at $y = \pm L$. The calculation of the response functions $\{\phi_q\}$ can easily be generalized to handle two confining surfaces by including the appropriate boundary conditions in Eqs. (5). If the distance $2L$ is very large, the copolymer orderings induced by the two surfaces are not coupled, and the middle of the film ($|y| \ll L$) is disordered, $\phi \approx 0$. Decreasing the film thickness to a distance comparable to the copolymer correlation length results in an overlap of the two surface fields.

Complex three dimensional morphologies can also be achieved by using only one dimensional surface patterns, if the two patterns are rotated with respect to each other. Such an example is shown in Fig. 5, for two surfaces at $y = \pm L = \pm d_0$ with perpendicularly oriented stripes. The surface patterns are shown in (a) and (c), while the mid-plane checkerboard morphology ($y = 0$) is shown in (b). In the next subsection we will show results for the more complicated situation of BCP melt below the ODT temperature, where the bulk phase is lamellar.

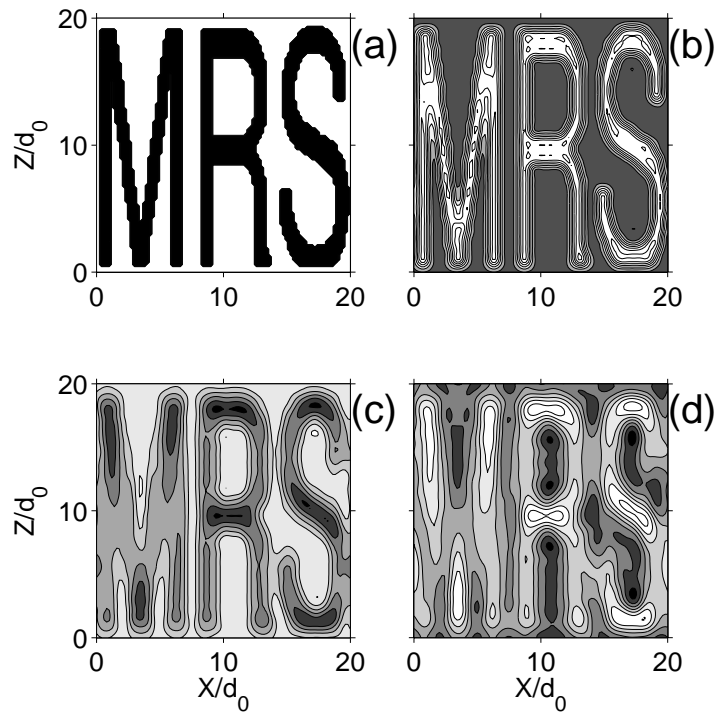


Figure 4. Propagation of surface order into the bulk BCP melt. (a) The surface at $y = 0$ is taken to have a pattern in the shape of the letters ‘MRS’. Inside the letters ($\sigma = 1$) the field attracts the B monomers, while the rest of the surface is neutral ($\sigma = 0$). In (b), (c) and (d) the morphology is calculated for $x-z$ planes located at increasing distances from the surface, $y/d_0 = 0.5, 2$ and 3.5 , respectively. Note that in (b) and (d) black (white) shades can be mapped into white (black) shades in (c), because their y -spacing is a half-integer number of lamellae. The Flory parameter is $\chi N = 9.5$.

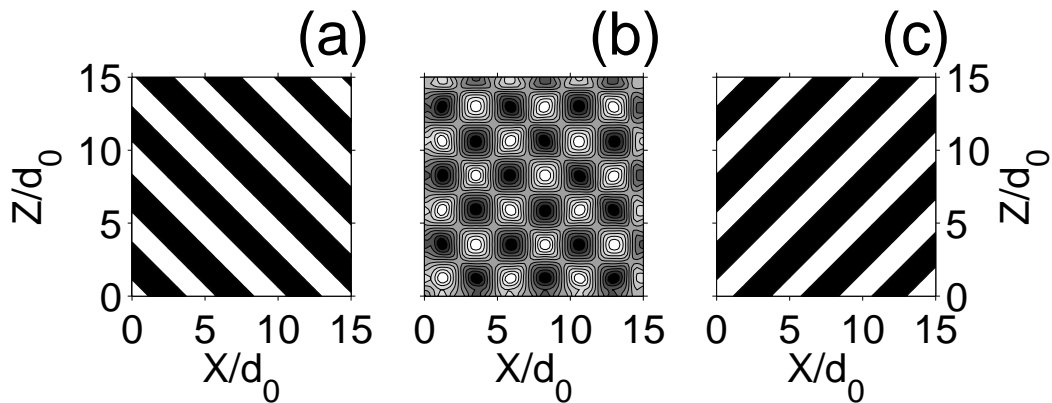


Figure 5. Creation of three dimensional structure in a thin BCP film as a result of two one-dimensional surface patterns. (a) and (c) are stripe surfaces located at $y = -L = -d_0$ and $y = L = d_0$, respectively. The mid-plane ($y = 0$) ordering is shown in (b) and is created by a superposition of the two surface fields. $\chi N = 9$.

Below ODT

The prevailing bulk phase below the ODT has an inherent lamellar ordering. This order

interferes strongly with the surface induced order, and it is not a simple task to obtain order-parameter expressions as a function of arbitrary surface pattern. Mathematically, the difficulty lies in the fact that the ϕ^4 term in the free energy cannot be neglected. As in the case above the ODT, we expand the free energy to second order around the bulk phase, only this time the bulk phase is lamellar. As we will see, this approach has also been used to describe defects in bulk phases such as chevron and omega-shaped tilt grain boundaries [26, 27]. We consider first a BCP melt confined by one stripe surface whose one dimensional pattern is of the form:

$$\sigma(x, z) = \sigma_q \cos(q_x x) \quad (6)$$

The surface periodicity $d_x = 2\pi/q_x$ is assumed to be larger than the bulk lamellar spacing $d_0 = 2\pi/q_0$, $d_x > d_0$ throughout the analysis. The system reduces its interfacial energy by trying to follow the surface modulations, and an overall tilt of the lamellae follows regardless of the fine details of chain conformations near the surface. The tilt angle with respect to the surface is defined as $\theta = \arcsin(d_0/d_x)$ [20]. Consequently, we use the single q -mode approximation to describe the bulk phase ϕ_b

$$\phi_b(x, y) = -\phi_q \cos(q_x x + q_y y) \quad (7)$$

where $q_y \equiv q_0 \sin(\theta)$ and $q_x = q_0 \cos(\theta)$. All surface effects are contained in the correction to the order parameter: $\delta\phi(\mathbf{r}) = \phi(\mathbf{r}) - \phi_b(\mathbf{r})$. We choose the in-phase one harmonic form for $\delta\phi$

$$\delta\phi(x, y) = g(y) \cos(q_x x) \quad (8)$$

with a y -dependent amplitude $g(y)$. This correction $\delta\phi$ is expected to vanish far from the surface, $\lim_{y \rightarrow \infty} \delta\phi = 0$, recovering the bulk phase. The free energy in Eq. (1) is expanded to second order in the small correction $\delta\phi$, $\phi_b \gg \delta\phi$. We integrate out the x dependence and retain only the y dependence. Then, use of a variational principle with respect to the function $g(y)$ yields a linear differential equation:

$$[A - C \cos(2q_y y)] g + Bg'' + g''' = 0 \quad (9)$$

where A , B , and C are parameters depending on the tilt angle θ as well as on the temperature [26]. This equation is similar to the Mathieu equation describing an electron under the influence of a periodic one-dimensional potential, and has a solution in the form of a Bloch wave function.

The main effect of the surface stripes on the melt is to introduce a tilt of the lamellae. This effect is seen in Fig. 6, where the surface periodicity d_x (in units of d_0) is chosen to be 1 in (a), and induces a perpendicular ordering. Larger ratios of d_x/d_0 cause a tilt ordering. In (b) $d_x/d_0 = 3/2$ and in (c) $d_x/d_0 = 3$, and the deviation from a perfect lamellar shape can be seen near the surface.

Tilt Grain Boundaries

Our approach can be used to describe defects in bulk systems as well. A tilt grain boundary forms when two lamellar bulk grains meet with a tilt angle φ between the lamellae normals. For symmetric tilt grain boundaries, the plane of symmetry is analogous to the patterned

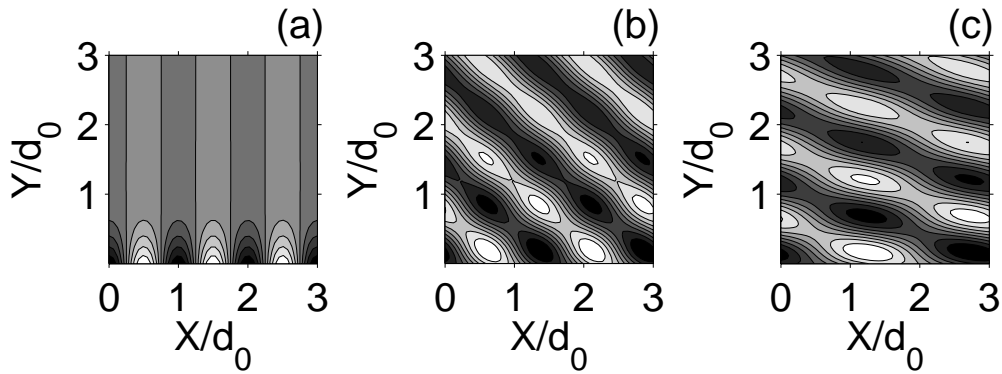


Figure 6. BCP melt confined by one stripe surface of periodicity $d_x > d_0$ below the ODT. The surface stripes are described by $\sigma(x) = \sigma_q \cos(q_x x)$. Tilted lamellae with respect to the surface at $y = 0$ are formed and adjust to the surface imposed periodicity. Far from the surface the lamellae relax to their undistorted d_0 spacing. The mismatch ratio d_x/d_0 is 1 in (a) yielding no tilt, $3/2$ in (b) and 3 in (c). The Flory parameter is taken as $\chi N = 10.6$ and $\sigma_q = 0.08$.

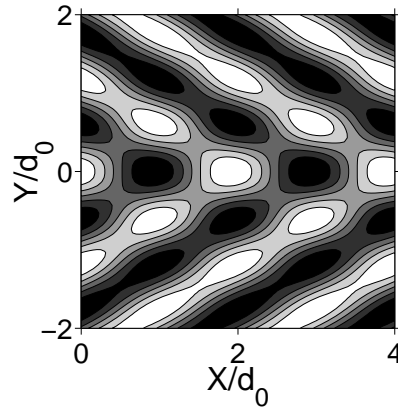


Figure 7. Symmetric tilt grain boundary between two bulk lamellar grains. The angle between lamellae is determined by external boundary conditions at $y \rightarrow \infty$ and is chosen here to be $\varphi = 120^\circ$. The morphology is invariant in the z direction and $\chi N = 11$.

surface in a thin BCP film, and similar form of a correction field $\delta\phi$ can be used, see Fig. 7. The upper half plane $y > 0$ thus corresponds to Fig. 6 (b) and (c).

The correction is small in the so-called chevron region (small tilt angle φ), but becomes important for larger tilt angles [26] where the grain boundary has the form of the letter Omega. Close to the ODT point the modulations at the interface become long range and persist into the bulk up to large distances. One of the differences between tilt grain boundaries and tilt induced by surface field is that in the former case there are no real surface fields. The tilt angle between adjacent grains is determined by constraints imposed far from the $y = 0$ interface.

CONCLUSIONS

An analytical expansion of the free energy, Eq. (1), can be used to obtain order parameter expressions for a BCP melt confined by one or two flat surfaces whose pattern has arbitrary (two dimensional) shape. The thin film morphology can also have a complex three dimensional form even if the two surfaces have one dimensional patterns with different orientations with respect to each other, see Fig. 5. A BCP melt close to and above the ODT point shows decaying oscillations of the local concentration towards the bulk disorder value. Our analysis shows that close to the ODT large surface spatial features can be transferred into the BCP bulk far from the surface, while small surface details are greatly damped.

Below the ODT, confinement of the melt by patterned surfaces with periodicity $d_x > d_0$ leads to a formation of a surface layer characterized by lateral periodicity of d_x , and the lamellae relax to their natural periodicity d_0 farther from the surface. The proposed mechanism is a tilting of the lamellae. We show that the resulting pattern have similar characteristics to bulk domain walls (tilt grain boundaries).

ACKNOWLEDGMENTS

We would like to thank M. Muthukumar, R. Netz, G. Reiter, T. Russell, M. Schick and U. Steiner for useful comments and discussions. Partial support from the U.S.-Israel Binational Foundation (B.S.F.) under grant No. 98-00429 and the Israel Science Foundation funded by the Israel Academy of Sciences and Humanities — centers of excellence program is gratefully acknowledged.

References

- [1] F. S. Bates and G. H. Fredrickson, *Annu. Rev. Phys. Chem.* **41**, 525 (1990).
- [2] K. Ohta and K. Kawasaki, *Macromolecules* **19**, 2621 (1986).
- [3] L. Leibler, *Macromolecules* **13**, 1602 (1980).
- [4] K. Binder, H. L. Frisch and S. Stepanow, *J. Phys. II* **7**, 1353 (1997).
- [5] G.H. Fredrickson and E. Helfand, *J. Chem. Phys.* **87**, 697 (1987).
- [6] M. W. Matsen and M. Schick, *Phys. Rev. Lett.* **72**, 2660 (1994); M. W. Matsen and F. Bates, *Macromolecules* **29**, 7641 (1996).
- [7] G. H. Fredrickson, *Macromolecules* **20**, 2535 (1987).
- [8] H. Tang and K. F. Freed, *J. Chem. Phys.* **97**, 4496 (1992).
- [9] K. R. Shull, *Macromolecules* **25**, 2122 (1992).
- [10] M. S. Turner, *Phys. Rev. Lett.* **69**, 1788 (1992).

- [11] M. S. Turner, M. R. Rubinstein and C. M. Marques, *Macromolecules* **27**, 4986 (1994).
- [12] M. W. Matsen, *J. Chem. Phys.* **106**, 7781 (1997).
- [13] S. H. Anastasiadis, T. P. Russell, S. K. Satija and C. F. Majkrzak, *Phys. Rev. Lett.* **62**, 1852 (1989).
- [14] A. Menelle, T. P. Russell, S. H. Anastasiadis, S. K. Satija and C. F. Majkrzak, *Phys. Rev. Lett.* **68**, 67 (1992).
- [15] D. G. Walton, G. J. Kellogg, A. M. Mayes, P. Lambooy and T. P. Russell, *Macromolecules* **27**, 6225 (1994).
- [16] G. J. Kellogg, D. G. Walton, A. M. Mayes, P. Lambooy, T. P. Russell, P. D. Gallagher and S. K. Satija, *Phys. Rev. Lett.* **76**, 2503 (1996).
- [17] P. Mansky, T. P. Russell, C. J. Hawker, J. Mayes, D. C. Cook and S. K. Satija, *Phys. Rev. Lett.* **79**, 237 (1997).
- [18] S. T. Milner and D. C. Morse, *Phys. Rev. E* **54**, 3793 (1996).
- [19] G. T. Pickett and A. C. Balazs, *Macromolecules* **30**, 3097 (1997).
- [20] D. Petera and M. Muthukumar, *J. Chem. Phys.* **107**, 9640 (1997); D. Petera and M. Muthukumar, *J. Chem. Phys.* **109**, 5101 (1998).
- [21] T. Geisinger, M. Mueller and K. Binder, *J. Chem. Phys.* **111**, 5241 (2000).
- [22] G. G. Pereira and D. R. M. Williams, *Phys. Rev. E* **60**, 5841 (1999); G. G. Pereira and D. R. M. Williams, *Phys. Rev. Lett.* **80**, 2849 (1998).
- [23] Y. Fink, J. N. Winn, S. Fan, C. Chen, J. Michael, J. D. Joannopoulos and E. L. Thomas, *Science* **282**, 1679 (1998).
- [24] S. Walheim, E. Schäffer, J. Mlynek and U. Steiner, *Science* **283**, 520 (1999).
- [25] M. Park, C. Harrison, P. M. Chaikin, R. A. Register and D. H. Adamson, *Science* **276**, 5317 (1997).
- [26] Y. Tsori, D. Andelman and M. Schick, *Phys. Rev. E.* **61**, 2848 (2000).
- [27] R. R. Netz, D. Andelman and M. Schick, *Phys. Rev. Lett.* **79**, 1058 (1997); S. Villain-Guillot, R. R. Netz, D. Andelman and M. Schick, *Physica A* **249**, 285 (1998); S. Villain-Guillot and D. Andelman, *Eur. Phys. J. B* **4**, 95 (1998).
- [28] J. Swift and P. C. Hohenberg, *Phys. Rev. A* **15**, 319 (1977).
- [29] M. Seul and D. Andelman, *Science* **267**, 476 (1995).
- [30] A. E. Jacobs, D. Mukamel and D. W. Allender, *Phys. Rev. E* **61**, 2753 (2000).

- [31] G. Gompper and M. Schick, *Phys. Rev. Lett.* **65**, 1116 (1990); F. Schmid and M. Schick, *Phys. Rev. E* **48**, 1882 (1993).
- [32] G. Gompper and S. Zschocke, *Phys. Rev. A* **46**, 1836 (1992).
- [33] D. Andelman, F. Brochard and J.-F. Joanny, *J. Chem. Phys.* **86**, 3673 (1987).
- [34] T. Garel and S. Doniach, *Phys. Rev. B* **26**, 325 (1982).
- [35] Y. Tsori and D. Andelman, *Macromolecules*, in press (2001).
- [36] Y. Tsori and D. Andelman, *Europhys. Lett.*, to be published (2001).
- [37] Y. Tsori and D. Andelman, *unpublished*.